Optical Engineering

OpticalEngineering.SPIEDigitalLibrary.org

Femtosecond laser-written lithium niobate waveguide laser operating at 1085 nm

Yang Tan
Javier R. Vázquez de Aldana
Feng Chen

SPIE.

Femtosecond laser-written lithium niobate waveguide laser operating at 1085 nm

Yang Tan,[a] Javier R. Vázquez de Aldana,[b] and Feng Chen[a,*]
[a]Shandong University, School of Physics, State Key Laboratory of Crystal Materials, and Key Laboratory of Particle Physics and Particle Irradiation (Ministry of Education), Jinan 250100, China
[b]Universidad de Salamanca, Laser Microprocessing Group, Departamento Física Aplicada, Salamanca 37008, Spain

Abstract. We report on the channel waveguide lasers at 1085 nm in femtosecond laser written Type II waveguides in an Nd:MgO:$LiNbO_3$ crystal. The waveguide was constructed in a typical dual-line approach. In the geometry, we found that four vicinal regions of the track pair could guide light propagation. In addition, these guiding cores support polarization-dependent-guided modes. The propagation losses of the waveguides were measured to be as low as 1 dB/cm. Under an optical pump at 808 nm, the continuous-wave waveguide lasing at 1085 nm was generated, reaching a slope efficiency of 27% and maximum output power of 8 mW. The lasing threshold was 71 mW. Our results show that with the femtosecond laser written Nd:MgO:$LiNbO_3$ waveguide as the miniature light source, it was possible to construct all-$LiNbO_3$-based integrated devices for diverse photonic applications. [DOI: 10.1117/1.OE.53.10.107109]

Keywords: optical waveguides; femtosecond laser writing; waveguide lasers; lithium niobate.

Paper 141299 received Aug. 16, 2014; revised manuscript received Sep. 24, 2014; accepted for publication Sep. 29, 2014; published online Oct. 23, 2014.

1 Introduction

Lithium niobate ($LiNbO_3$) is one of the most favorite materials for optical and photonic applications due to the combination of many excellent features related to the electro-optic, acousto-optic, and nonlinear optical responses.[1] These intriguing properties enable $LiNbO_3$ crystals to be very suitable substrates as the platforms for electrooptic modulators, surface-acoustic wave devices, holographic storage, and frequency converters.[2–4] Recently, it has been proven that $LiNbO_3$ could also serve as a key element in the generation of entangled photon pairs for quantum photonics.[5] Codoped by neodymium (Nd) and magnesium (Mg) ions, $LiNbO_3$ become a promising gain medium Nd:MgO:$LiNbO_3$ for laser generation with a relatively high optical damage threshold.[6] The $LiNbO_3$-based devices have attracted much attention and most of them are constructed on waveguide platforms.[3] Optical waveguides are the fundamental elements in integrated optics.[7–9] Compared with the bulk configuration, the light confined in waveguides possesses relatively high optical intensities due to the very small volumes of the guiding cores.[9] Some $LiNbO_3$-based devices have become commercially available, such as optical modulators, frequency doublers (with periodically poled $LiNbO_3$, PPLN), optical amplifiers, and so on. Due to the highly compressed intracavity intensity, waveguide lasers possess reduced lasing thresholds and comparable efficiencies with respect to bulk lasers.[7] Optical waveguides have been fabricated in various LN substrates by using a few techniques such as metal ion indiffusion (Ti, Zn, or Fe), proton exchange, energetic ion implantation/irradiation, and femtosecond laser writing.[10–17] Since 1996, when Davis et al.[18] first produced waveguides in glass by direct femtosecond laser writing, this technique has become a powerful tool with which to fabricate optical waveguides in various transparent optical materials.[19–24] Particularly, waveguides with diverse geometries have been fabricated in $LiNbO_3$ crystals by using the inscription of ultrafast pulses.[15–17,25,26] It has been revealed that, for $LiNbO_3$ crystals, the femtosecond laser-induced refractive index changes in the damaged track region could be either positive or negative, depending on the parameters of the laser beams and the crystalline orientations of the samples. Positive index changes are only available for an extraordinary index (n_e), in which the weak damage induced by the femtosecond laser pulses on the lattice is dominant.[15] In this case, the waveguide core is located just inside the femtosecond laser written track due to the slight increment of n_e, forming a Type I waveguide configuration. In most cases, femtosecond lasers induce negative index changes inside the damaged tracks, and for $LiNbO_3$, both the extraordinary refractive index and the ordinary refractive index (n_o) will decrease due to the induced severe damage of the lattices (usually with a volume expansion) inside the track cores. Meanwhile, in the surrounding regions of the low-index tracks, the refractive index may increase due to the stress-field effect (caused by the lattice compression), forming guiding cores. For typical Type II waveguides with dual-line geometry, the main waveguiding core is located in the region between two parallel tracks. However, for strongly birefringent crystals such as $LiNbO_3$, the refractive index modifications in the vicinity of the tracks are more complicated and have obvious polarization-dependent effects.[15] Moreover, from the application point of view, one could integrate gain medium, nonlinear components and electrooptic modulators in a single laser-written chip, realizing hybrid and multifunctional circuits based on $LiNbO_3$ platforms.[17] To date, the integration of femtosecond laser written nonlinear PPLN and $LiNbO_3$ modulators has been achieved,[17] while a laser source based on a femtosecond laser written $LiNbO_3$ is

*Address all correspondence to: Feng Chen, E-mail: drfchen@sdu.edu.cn

absent. In this work, we have investigated the guiding effect of the femtosecond laser written dual-line Type II structures in an $Nd:MgO:LiNbO_3$ crystal, and realized waveguide lasing from the structure at 1085 nm under an optical pump of 808 nm.

2 Experiments in Details

The y-cut $Nd:MgO:LiNbO_3$ (doped with 0.3 at.% Nd^{3+} ions and 5 mol% MgO) crystal was cut into dimensions of $7(x) \times 2(y) \times 10(z)$ mm^3 and optically polished. The Type II structure was fabricated by femtosecond laser writing in the laser facility of the Universidad de Salamanca, Spain. A Ti:Sapphire regenerative amplifier (Spitfire, Spectra Physics, USA) was used as laser source to deliver linearly polarized laser pulses of 120 fs and a 795-nm central wavelength at a 1-kHz repetition rate. The maximum pulse energy was 1 mJ. The energy was reduced with a calibrated neutral density filter placed after a half-wave plate and a linear polarizer in order to get fine control of the incident energy before the laser reached the sample. The laser beam was focused at a depth of ~500 μm below the biggest facet through a 10× microscope objective and inscribed the pair of parallel tracks along the x axis with a 20-μm lateral separation inside crystal. The scanning rate of the laser beam was 50 μm/s. Figure 1(a) shows the experimental schematic with the crystalline orientation. Figure 1(b) depicts the cross-sectional microscopic image of the dual-line structure. In this image, four regions are labeled as A, B, C, and D, which indicate the vicinal regions of the damaged track pair. The guiding properties of the structure at A, B, C, and D regions were investigated with an end-face coupling system with a laser operating at a wavelength of 808 nm. The details of such an arrangement can be referenced elsewhere.[15]

A continuous wave Ti:Sapphire laser (Coherent MBR PE, USA) which generated a polarized light pump beam at 808 nm was used in the end pumping system to perform the waveguide laser operation experiment. A spherical convex lens with a focal length of 25 mm was used to couple the pump laser beam into the waveguide. Two mirrors (M1 and M2) were adhered to the sample to form a Fabry–Perot waveguide laser resonant cavity (see Fig. 2 for schematic plot). The input mirror M1 had a transmission of 99% at 808 nm and a reflectivity of 99% at 1085 nm. The output mirror M2 had a 60% reflectivity at 1085 nm and a 99% reflectivity at 808 nm. The output light was collected by a 20× microscope objective lens (N.A. = 0.4) and its spectra were analyzed by a spectrometer with 0.2-nm resolution. Two power meters were utilized to measure the powers of the launched and output lasers through the waveguide cores.

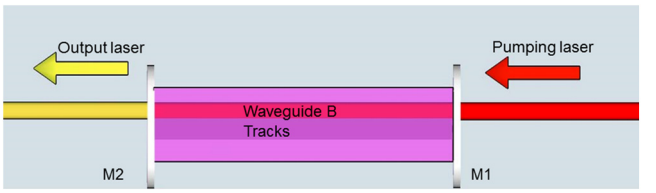

Fig. 2 The schematic of the laser cavity based on the femtosecond laser written dual-line structure in a $Nd:MgO:LiNbO_3$ crystal.

3 Results and Discussion

Figures 3(a)–3(d) show the measured mode profiles at a wavelength of 808 nm for the structure at the A, B, C, and D regions, respectively. The propagation loss of the waveguides was measured by the technique demonstrated in Ref. 27. The propagation loss for each waveguide is 2.0 dB/cm [Fig. 3(a)], 1.5 dB/cm [Fig. 3(b)], and 1.5 dB/cm [Figs. 3(c) and 3(d)], respectively. Thermal annealing treatment of the sample at 300 to 400°C for 1 h could further reduce the loss values by ~0.5 dB/cm. As we can see, the guided modes were observed in all four regions, indicating effective guidance of the structure. However, we have found that the guidance of the four regions was strongly polarization dependent. In regions A, C, and D, i.e., in the region between the two tracks and the two outsides of the tracks, only the TM-polarized light can propagate and the TE mode does not exist. This means the waveguide cores in A, C, and D guide light along the n_o axis. On the contrary, in the region of B, i.e., above the two track lines, we only observed the TE mode with n_e polarization. The relationship of polarization and waveguide position can be explained with the mechanism of ultrafast laser writing through the stress-induced effect.[15] The refractive index change could be approximately expressed by Eq. (1),

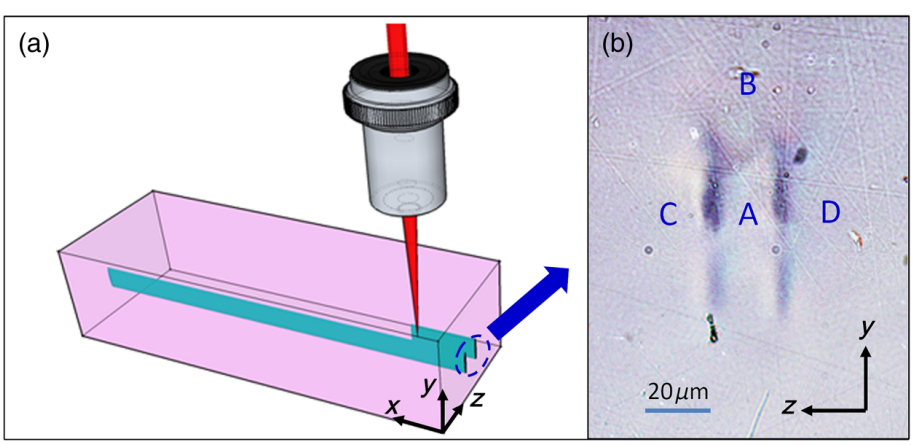

Fig. 1 (a) The schematic plot of femtosecond laser written dual-line structure in a $Nd:MgO:LiNbO_3$ crystal; (b) the cross-sectional microscope image of the dual-line structure. A to D mark the four special regions of the structure.

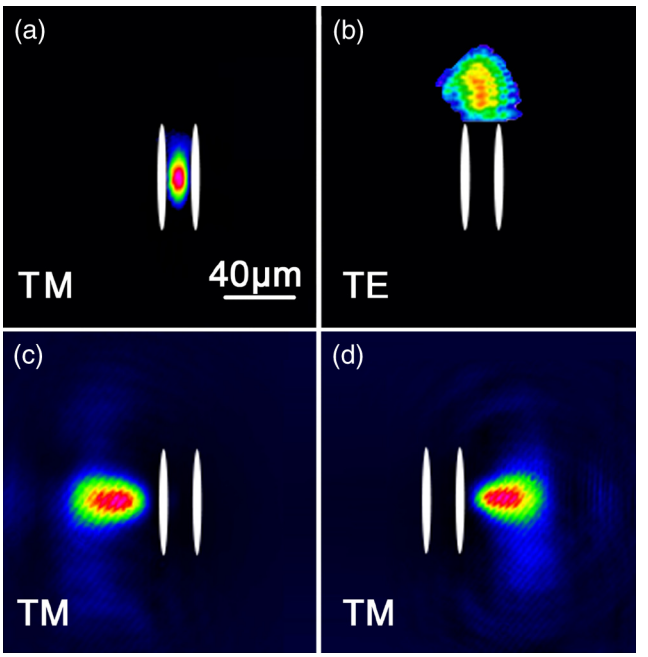

Fig. 3 The measured mode profiles (intensity distribution) of waveguide cores A, B, C, and D, corresponding to (a), (b), (c), and (d), in the Nd:MgO:$LiNbO_3$ crystal. The white shadows show the spatial locations of the track pair.

$$\Delta\left(\frac{1}{n^2}\right)_{ij} = \sum_{k,l} \pi_{ijkl}\sigma_{kl}, \tag{1}$$

where π_{ijkl} is piezooptic tensor; σ_{kl} is the stress. The result of refractive index change could be derived from Eq. (1).[15] At the sides of the tracks, the induced stress is along the y axis (vertical direction), resulting in an increment of n_o (corresponding to the TM polarization). In addition, the n_e (corresponding to the TE polarization) increases above and below the tracks due to the horizontal induced-stress field.[15] This means that, in the regions of A, C, and D, the n_o increases, and in B, the n_e increases, resulting in waveguide cores. In addition, no guiding effect was found in the region below the track pairs, which may be due to the fact that the fabricated structure did not have perfectly symmetrical geometry along the vertical direction.

The laser experiments were carried out with an end-pumping configuration. It was found that although the guidance exists in all four regions, waveguide lasing was only generated in region B. From the inset of Fig. 4, the emission spectrum shows a sharp peak (with full width at half maximum ~1.5 nm) at 1085 nm, which corresponds to the wavelength of the main fluorescence of $^4F_{3/2} \rightarrow {}^4I_{11/2}$ transition lines related to the Nd^{3+} ions. This wavelength of the laser emissions is in good agreement with that of the Nd:MgO:$LiNbO_3$ bulk.[6] Figure 4 shows the output laser power from the waveguide core B as a function of the absorbed pump power at 808 nm. From this figure, one can determine the lasing threshold and the slope efficiency are ~71 mW and ~27%, respectively. The output laser power reached its maxima of 8 mW when the absorbed pump power was 100 mW.

It should be noted that waveguide lasing cannot be generated in the waveguide cores of A, C, and D under the maximum absorbed pump power of our system (i.e., ~100 mW).

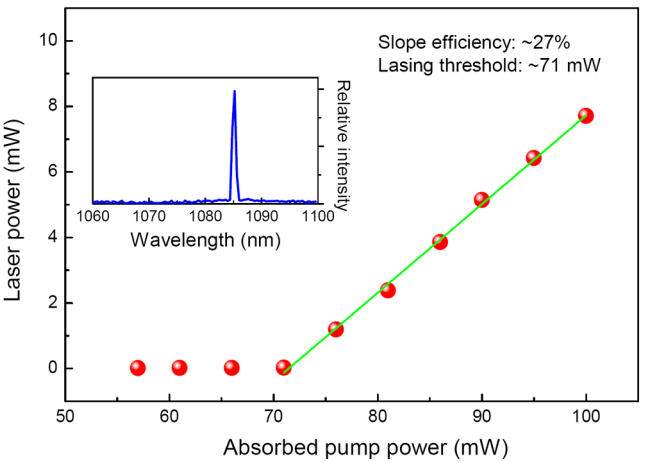

Fig. 4 The output power of the waveguide laser at 1085 nm as a function of the absorbed pump power at 808 nm. The inset shows the laser oscillation spectrum from the waveguide core B after pump power above the threshold.

This means that the lasing threshold through the waveguide cores of A, C, and D may be much higher than the waveguide core of region B. The threshold difference can be explained based on the fluorescence properties of a Nd:MgO:$LiNbO_3$ crystal.[10] As a four-level system laser, the threshold power is inversely proportional to the emission cross section. For the Nd:MgO:$LiNbO_3$ crystal, the cross section along the z axis is much larger than that along the x and y axes. This property means that lasing can only occur for n_e polarized light in bulk crystal. In the present work, the guided light in cores A, C, and D was with TM polarization, corresponding to the n_o orientation, and in core B it was with the TE polarization of the n_e axis. Such a geometry with bulk features results in waveguide lasing in the region above the track pair. One could expect that with a z-cut Nd:MgO:$LiNbO_3$ sample, the waveguide lasers could be generated in regions A, C, and D.

4 Summary

We have reported on the waveguiding lasing of a femtosecond laser inscribed x-cut Nd:MgO:$LiNbO_3$ dual-line structure. The generated laser was with TE polarization, which was along the n_e axis of the crystal. Under the 808-nm excitation, the waveguide laser has shown an acceptable performance with a slope efficiency of 27% and a threshold of 71 mW.

Acknowledgments

The work was supported by the National Natural Science Foundation of China (No. 11274203), the Specialized Research Fund for the Doctoral Program of Higher Education of China (No. 20130131130001), and Junta de Castilla y León under project SA086A12-2. Support from the Centro de Láseres Pulsados (CLPU) was also acknowledged.

References

1. L. Arizmendi, "Photonic applications of lithium niobate crystals," *Phys. Status Solidi A* **201**(2), 253–283 (2004).
2. K. Buse, A. Adibi, and D. Psaltis, "Non-volatile holographic storage in doubly doped lithium niobate crystals," *Nature* **393**(6686), 665–668 (1998).
3. W. Sohler et al., "Integrated optical devices in lithium niobate," *Opt. Photonics News* **19**(1), 24–31 (2008).

4. E. L. Wooten et al., "A review of lithium niobate modulators for fiber-optic communications systems," *IEEE J. Sel. Top. Quantum Electron.* **6**(1), 69–82 (2000).
5. S. Tanzilli et al., "On the genesis and evolution of integrated quantum optics," *Laser Photonics Rev.* **6**(1), 115–143 (2012).
6. A. Cordova-Plaza et al., "Nd:MgO:$LiNbO_3$ continuous-wave laser pumped by a laser diode," *Opt. Lett.* **13**, 209–211 (1988).
7. C. Grivas, "Optically pumped planar waveguide lasers, Part I: Fundamentals and fabrication techniques," *Prog. Quantum Electron.* **35**(6), 159–239 (2011).
8. E. J. Murphy, *Integrated Optical Circuits and Components*, Marcel Dekker, New York (1999).
9. F. Chen and J. R. V. de Aldana, "Optical waveguides in crystalline dielectric materials produced by femtosecond-laser micromachining," *Laser Photonics Rev.* **8**(2), 251–275 (2014).
10. D. Jaque, E. Cantelar, and G. Lifante, "Lattice micro-modifications induced by Zn diffusion in Nd:$LiNbO_3$ channel waveguides probed by Nd^{3+} confocal micro-luminescence," *Appl. Phys. B* **88**(2), 201–204 (2007).
11. S. Mignoni et al., "Micro-Raman analysis of Fe-diffused lithium niobate waveguides," *Appl. Phys. B* **101**(3), 541–546 (2010).
12. P. Baldi et al., "Proton exchanged waveguides in $LiNbO_3$ and $LiTaO_3$ for integrated lasers and nonlinear frequency converters," *Opt. Eng.* **37**(4), 1193–1202 (1998).
13. C. Becker et al., "Advanced Ti:Er:$LiNbO_3$ waveguide lasers," *IEEE J. Sel. Top. Quantum Electron.* **6**(1), 101–113 (2000).
14. F. Chen, "Photonic guiding structures in lithium niobate crystals produced by energetic ion beams," *J. Appl. Phys.* **106**(8), 081101 (2009).
15. J. Burghoff, S. Nolte, and A. Tunnermann, "Origins of waveguiding in femtosecond laser-structured $LiNbO_3$," *Appl. Phys. A* **89**(1), 127–132 (2007).
16. R. He et al., "Femtosecond laser micromachining of lithium niobate depressed cladding waveguides," *Opt. Mater. Express* **3**(9), 1378–1384 (2013).
17. J. Thomas et al., "Laser direct writing: enabling monolithic and hybrid integrated solutions on the lithium niobate platform," *Phys. Status Solidi A* **208**(2), 276–283 (2011).
18. K. M. Davis et al., "Writing waveguides in glass with a femtosecond laser," *Opt. Lett.* **21**(21), 1729–1731 (1996).
19. J. Siebenmorgen et al., "Femtosecond laser written stress-induced Nd:$Y_3Al_5O_{12}$ (Nd:YAG) channel waveguide laser," *Appl. Phys. B* **97**(2), 251–255 (2009).
20. F. M. Bain et al., "Ultrafast laser inscribed Yb:$KGd(WO_4)_2$ and Yb:$KY(WO_4)_2$ channel waveguide lasers," *Opt. Express* **17**(25), 22417–22422 (2009).
21. C. Zhang et al., "Channel waveguide lasers in Nd:GGG crystals fabricated by femtosecond laser inscription," *Opt. Express* **19**(13), 12503–12508 (2011).
22. M. Ams et al., "Ultrafast laser written active devices," *Laser Photonics Rev.* **3**(6), 535–544 (2009).
23. G. Salamu et al., "Cladding waveguides realized in Nd:YAG ceramic by direct femtosecond-laser writing with a helical movement technique," *Opt. Mater. Express* **4**, 790–797 (2014).
24. D. G. Lancaster et al., "Fifty percent internal slope efficiency femtosecond direct-written Tm^{3+}:ZBLAN waveguide laser," *Opt. Lett.* **36**(9), 1587–1589 (2011).
25. Y. Liao et al., "Electro-optic integration of embedded electrodes and waveguides in $LiNbO_3$ using a femtosecond laser," *Opt. Lett.* **33**(19), 2281–2283 (2008).
26. H. T. Bookey et al., "Femtosecond laser inscription of low insertion loss waveguides in Z-cut lithium niobate," *IEEE Photonics Technol. Lett.* **19**(12), 892–894 (2007).
27. L. Wang et al., "Low-loss planar and stripe waveguides in Nd^{3+}-doped silicate glass produced by oxygen-ion implantation," *J. Appl. Phys.* **101**(5), 053112 (2007).

Yang Tan received his bachelor's degree (2006) from Shandong Normal University and PhD (2011) from Shandong University, China. He is currently a lecturer at the School of Physics, Shandong University. His current research interests include fabrication of optical waveguides in laser materials by using ion implantation and femtosecond laser inscription.

Javier R. Vázquez de Aldana received his Bachelor of Science degree (1997) and his PhD (2001) from the University of Salamanca, Spain. He is currently an associate professor of the Science Faculty, University of Salamanca, Spain. His research activity is focused on the interaction of intense femtosecond pulses with materials and its application to fabrication of photonic devices. He is a member of the Laser Microprocessing Research Group, and is also a technical and scientific advisor of the Laser Facility at University of Salamanca.

Feng Chen is a professor and dean of the School of Physics, Shandong University, China. He received his PhD degree from Shandong University in 2002. He was a Humboldt Fellow from 2003 to 2005. His interests include material modifications by ultrafast lasers and ion beams, optical waveguides, etc. He has published ~200 papers in peer-reviewed journals. He is a fellow of IOP, a senior member of OSA, and a member of SPIE. He serves as an associate editor of *Optical Engineering*.